Advanced benchmark of the flow through a mixing vane grid - Large Eddy Simulation validation

Benjamin Farges, Marie-Charlotte Gauffre, Sofiane Benhamadouche, Pierre Badel, Vincent Faucher, Guillaume Ricciardi

Advanced benchmark of the flow through a mixing vane grid – Large Eddy Simulation validation

Farges Benjamin
Framatome
10 rue Juliette Récamier, Lyon, FR-69006
benjamin.farges@framatome.com

Gauffre Marie-Charlotte
EDF
19 Rue Pierre Bourdeix, 69007 Lyon
marie-charlotte.gauffre@edf.fr

Benhamadouche Sofiane
EDF Lab
6 quai Watier, Chatou, FR-78400
sofiane.benhamadouche@edf.fr

Badel Pierre
EDF Lab
Boulevard Gaspard Monge, 91120 Palaiseau
Pierre-bernard.badel@edf.fr

Faucher Vincent*
CEA, DES, IRESNE, Nuclear Technology Department,
Center of Cadarache, Saint-Paul-lez-Durance, FR-13108
vincent.faucher@cea.fr

Ricciardi Guillaume
CEA, DES, IRESNE, Nuclear Technology Department,
Center of Cadarache, Saint-Paul-lez-Durance, FR-13108
guillaume.ricciardi@cea.fr

ABSTRACT

Identifying what causes fuel assembly vibrations downstream of Mixing Vane Grids (MVG) in Pressurized Water reactor (PWR) is of paramount importance for nuclear community to understand grid-to-rod fretting wear. Experiments, called CALIFS, were carried out by the Atomic Energy Commission (CEA) on a 5x5 MVG at a hydraulic Reynolds number of 66,000, in order to measure the flow velocity and the pressure along the central rod. In parallel, a benchmark for Large Eddy Simulation (LES) was setup to compare the predictions of three different CFD codes: Star-CCM+, *Code_Saturne* and TrioCFD to experimental measurements. The computational domain is representative of a span of CALIFS mockup, composed of a 5x5 rod bundle with a MVG. The three computations overall give very satisfactory results, independently from the mesh created and the modelling options selected. It seems to suggest that whatever the software used, this kind of calculations has reached a significant level of robustness and accuracy. Nonetheless, some discrepancies remain concerning the predictions of pressure standard deviation decay far downstream of the mixing vane grid.

KEYWORDS

Pressurized Water Reactor fuel assembly, 5x5 mixing vane grid, CALIFS experiment, CFD benchmark, Large Eddy Simulation, pressure standard deviation.

1 INTRODUCTION: INDUSTRIAL CHALLENGE AND PURPOSE OF THE PAPER

Flow-induced vibrations (FIV) are a major research topic for nuclear reactor technology in general, and for the Pressurized Water Reactors in particular. Beyond the need to always prevent fluidelastic instability phenomena which could lead to rapid failures, it is also necessary to account for the long-time effects of the flow turbulence excitations. For instance, the grid-to-rod fretting wear is still a worldwide dominant fuel rod leaker mechanism [1] and its main cause has been identified as fuel rod vibration induced by the turbulent flow [2].

This topic is currently tackled through dedicated experiments. Carrying out the associated simulation is still a challenging field for *Computational Fluid Dynamics* (CFD) software due the stochastic and turbulence-induced nature of the fluid loading applied to the structures at rod/grid level within a fuel assembly. Benhamadouche et al. [11] carried out wall-modelled LES of the flow through a 4x4 mixing vane grid at a Reynolds number of 40,000, in order to compute the pressure load. This latter has been used combined to a beam equation to predict the displacements obtained along a rod and the qualitative results corresponded

to what is observed in reality (few microns). However, this computation cannot be considered as validated and the methodology has to be confronted to experimental data. A dedicated Round Robin exercise to the flow through Simple Support Grids and Mixing Vane Grids has been carried out by EPRI [12]. This benchmark included heat transfer. Almost only RANS models have been employed in this benchmark and the ability to capture pressure fluctuations has not been addressed.

Many recent attempts to simulate the fluid flow in a fuel assembly can be found in the literature. Bieder et al. [16] showed that, downstream close to the mixing vane the turbulence is isotropic and anisotropic further downstream. Chen et al. in [17] showed that simulation should count at least a 4 by 4 rod bundle to represent a full bundle. The turbulent intensity generated by the mixing vanes is underestimated by standard *k-epsilon* simulations [18], LES simulation perform better especially far from the grid [19]. The design of mixing van has as strong influence on the turbulence [20], more specifically the inclination of the vanes increases the turbulent intensity [21]. Spring and dimple have also an influence on the flow [22]. The MATiS-H benchmark conducted by KAERI showed that simulation accounting for LES model with the finest mesh does not guarantee the best results [23].

The purpose of the present article is to contribute to the definition of the state-of-the-art for industrial CFD computation of single phase highly turbulent flow in rod bundles involving mixing grids. A particular focus is dedicated to pressure fluctuations. The work involves cross-comparisons of predictions provided by three different CFD solvers with various user-environment and objectives as well as various implemented numerical methods and models for the case of interest, all evaluated with respect to a reference experiment named CALIFS (see for instance [3] and [4]) described further in this introduction.

Such a benchmark, with results produced mobilizing a significantly high level of expert knowledge in the use of each of considered software, is able to provide relevant insights regarding the capabilities of turbulent CFD simulation going far beyond the proposed application and contribute to the definition of design processes increasingly involving numerical results, with mandatory uncertainty assessment obtained from detailed calculation at local scale.

2 DESCRIPTION OF THE CALIFS 5X5 REFERENCE EXPERIMENT

CALIFS 5x5, illustrated in Figure 1, is a water rig working within the ranges 0-400 m3/h, 10°-70°C, 0-10 bars. The length of the test section is about 2.5 m. The flow cross section is a square of 184mm side. A 5x5 rods bundle, using rods of diameter 26.9 mm, is placed within the test section using spacer-grids, with one grid of interest with full optical access (see Figure 1-c and Figure 1-d). The hydraulic diameter (denoted D_h

in the following) of the bundle is 27.7 mm and is used as the reference length scale. The scale of the experiment is higher than 1 is order to use appropriate sensors to measure the pressure along the rods.

The grids are made with 1.2mm thick plates of stainless steel 304L. The height of the plates is 93 mm and they are assembled perpendicularly to design a mesh with 25 cells. Within each cell, the rods are sustained radially using dimples and springs-blades, representative of a realistic Mixing Vane Grid (MVG). The dimples are made of TEFLON[1] and the springs-blades are made with 1 mm thick blades of stainless steel 301 T4.

(a) General view of CALIFS 5x5 test rig

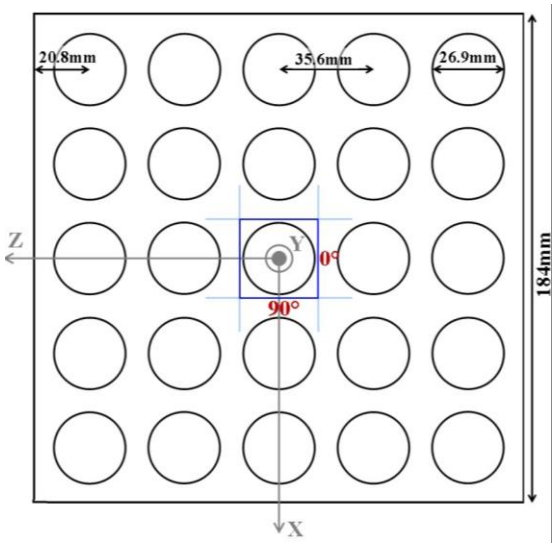

(b) Main dimensions and orientations

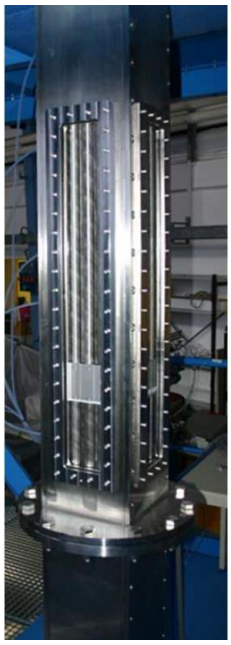

(c) View of the test section

[1] TEFLON is a registered trademark of E. I. du Pont de Nemours and Company or its affiliates.

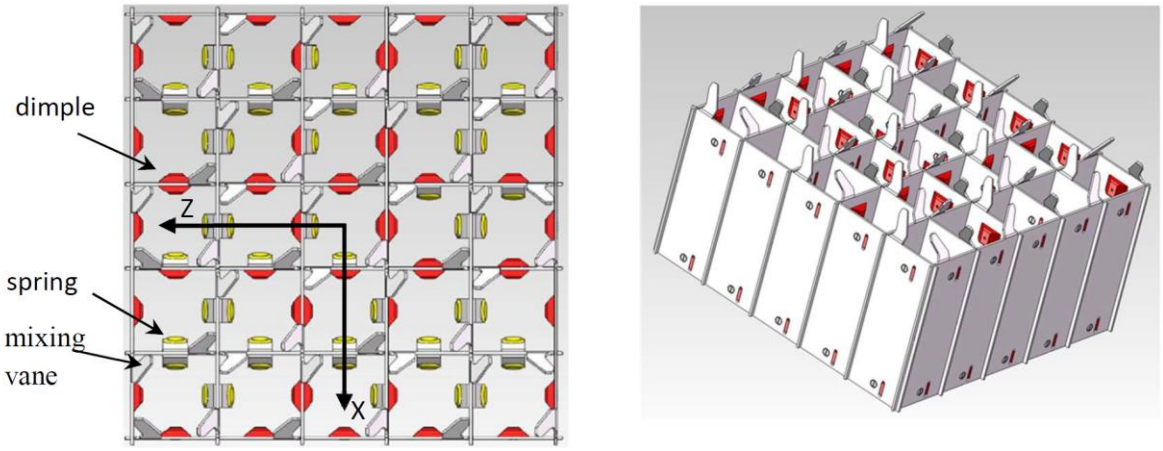

(d) View of the details of the mixing grid equipped with vanes

Figure 1. Some details about the CALIFS 5x5 reference experiment

The tests are performed for a flow rate velocity of 2.4 $m.s^{-1}$ and a flow temperature of 20°C, yielding a reference hydraulic Reynolds number of 66,000, enough to significantly challenge the simulation results in the turbulent regime.

Global pressure drops along the bundle and unsteady local pressure measurements are implemented, the latter being obtained by instrumenting the central rod of the 5x5 rods bundle with a high-resolution piezo-resistive sensor. The pressure distribution around the central rod circumference is obtained by turning the instrumented rod with an increment of 10° over 360°. This azimuthal distribution is measured at various longitudinal positions downstream of the grid of interest by translating the instrumented rod. The longitudinal distances which are studied are $0.5D_h$, $1D_h$, $2D_h$, $3D_h$, $4D_h$, $5D_h$, $10D_h$, $15D_h$ and $20D_h$ downstream of the mixing grid, respectively. Figure 2 shows an example extracted from [4] of the experimental distribution of pressure standard deviation against which numerical results will be evaluated. Only the red curves are considered in the present paper, the blue curves being obtained with a preliminary configuration without mixing vanes.

Average velocity profiles in the tube bundle are also provided through Laser Doppler Velocimetry (LDV) to serve also as experimental references for numerical results evaluation.

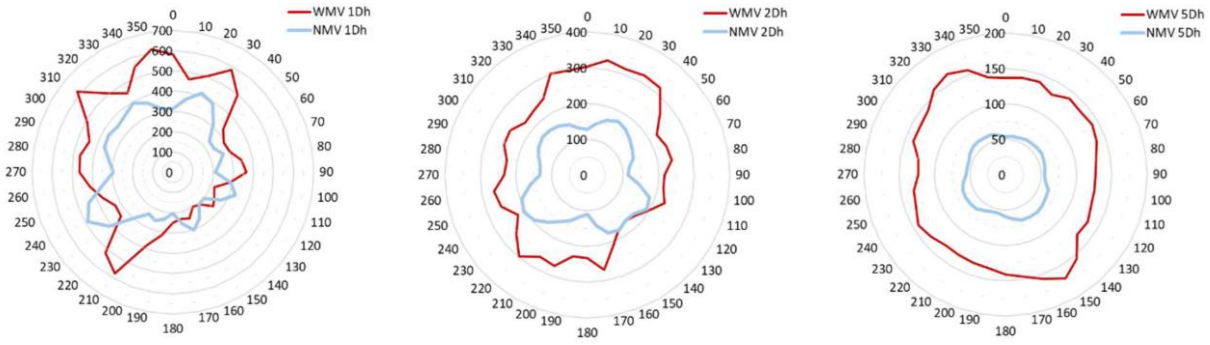

(a) $1D_h$ downstream of the MVG (b) $2D_h$ downstream of the MVG (c) $5D_h$ downstream of the MVG

Figure 2. Pressure standard deviation obtained in CALIFS 5x5 experiment at different distances from the mixing vane grid along the central rod (only the red curves have to be considered, the blue curves were obtained with a preliminary configuration without mixing vanes)

3 NUMERICAL MODELS

Since the purpose of the benchmark was to challenge and compare complete numerical simulations strategies for highly turbulent flow in a bundle configuration, numerical models mimicking CALIFS 5x5 experiment were built separately by Framatome, EDF and CEA using their usual solvers with their state of the art of expertise. The selected CFD programs are given in Table 1.

Framatome	Star-CCM+ V11.2 (https://www.plm.automation.siemens.com/global/fr/products/simcenter/Star-CCM.html) A fully industrial software solution from SIEMENS for design and engineering, including advanced CFD and co-simulation. [2]
EDF	*Code_Saturne* V5.0 (https://www.code-saturne.org/) A highly customizable open-source software for single phase laminar or turbulent flows developed by EDF, for many kinds of applications in the field of energy including in-core hydraulics for nuclear, external atmospheric flows and flows interacting with rotors within steam turbine.
CEA	TrioCFD (http://triocfd.cea.fr) A multi-purpose research open-source solution developed by CEA to provide high-resolution solutions for complex flows with interfaces, laminar or turbulent and designed for advanced multiphysical applications and couplings.

Table 1. Selected software for Framatome, EDF and CEA

The use of Large Eddy Simulation (see for instance [5] or [11]) for turbulence modelling was however imposed for all contributions, following the results obtained from previous work on a simplified yet representative configuration with one single rod inside one grid cell placed in a turbulent annular flow (see [6]).

3.1 Computational domain and boundary conditions

The characteristics of the computational domains considered by Framatome, EDF and CEA respectively are given in Figure 3.

[2] Star-CCM+® and any and all SIEMENS brand, product, service and feature names, logos and slogans are registered trademarks or trademarks of SIEMENS in the United States or other countries. All other brand, product, service and feature names or trademarks are the property of their respective owners

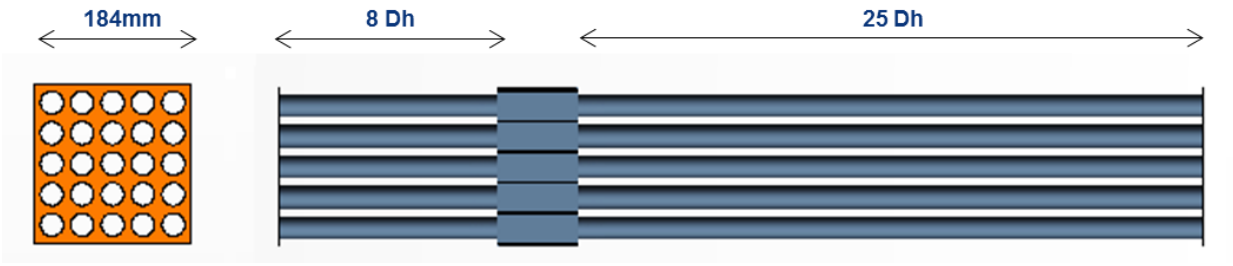

(a) Framatome computational domain, extending from $8D_h$ upstream the mixing grid of interest to $25D_h$ downstream, periodic boundary conditions are applied

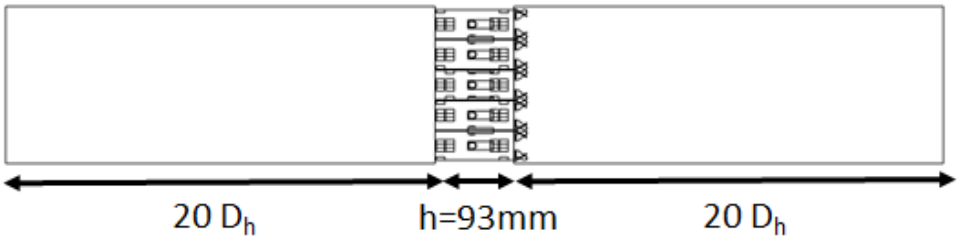

(b) EDF computational domain, extending from $20D_h$ upstream the mixing grid of interest to $20D_h$ downstream, implicit periodic boundary conditions are applied

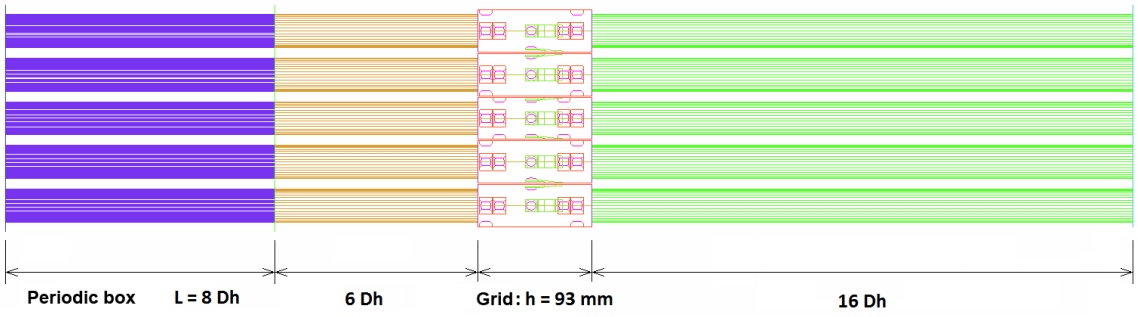

(c) CEA computational domain, extending from $6D_h$ upstream the mixing grid of interest to $16D_h$ downstream, and implementing a specific periodic box for turbulent inlet

Figure 3. Computational domains for Framatome, EDF and CEA

For Framatome, the periodicity is achieved by mapping of the flow field (pressure and velocity) between inlet and outlet to simulate periodic conditions. This mapping operation consists in extracting a set of data from a given boundary surface (velocity or pressure field, for instance) in order to set it to another boundary. This yields a three-phase calculation sequence:

- Phase 1: without any periodic condition, a constant velocity profile is set at the inlet and a constant pressure profile is set at the outlet. This phase lasts 5 flow passes ;

- Phase 2a: the mapped velocity is set at the inlet but the pressure boundary conditions remains unchanged. This phase lasts 5 flow passes;
- Phase 2b: the mapped pressure profile is set at the outlet. Both periodicity conditions are set. This phase lasts 5 flow passes;
- Phase 3: after solution stabilization of the first phases, data is collected after 15 flow passes.

For EDF, periodic conditions of translation are used in the stream-wise direction, with an imposed pressure gradient calculated from the flow rate.

CEA suggests a different approach with the initialization of the turbulent velocity field at the bottom entry of the domain ($6D_h$ upstream of the grid) obtained through a so-called periodic recirculation box (beginning $8D_h$ upstream of the bottom entry), where the bundle turbulence is fully established and from which the velocity conditions are extracted and imposed at each time step at the inlet of the physical domain. Pressure is imposed at the domain outlet.

In order to perform industrial and affordable computations, wall-modeled LES is used, especially by EDF and CEA (see below for the particular case of Framatome). This approach might give correct mean values (see Benhamadouche [13]). However, its use is still subject to discussion and objections (see Piomelli [14]) and this approach using wall functions concepts can also be seen as a very first step of hybrid RANS/LES technique (using a logarithmic profile for example). Table 2 describes the boundary conditions considered along the walls.

Framatome	EDF, CEA
So-called *all-y^+* approach from Star-CCM+, where the viscous sublayer is fully resolved for low y^+ (a standard wall law is applied for high y^+) This approach benefits from a specifically refined mesh of the boundary layer along the internal walls (see Paragraph 2.2 for meshing processes).	A classical logarithmic wall function is used to predict the wall shear stress and is active on each wall computational cell : $\begin{cases} \frac{U_I}{u^*} = \frac{1}{\kappa} ln(y^+) + E \quad \text{if } y^+ > 11.8 \\ \frac{U_I}{u^*} = y^+ \text{ otherwise} \end{cases}$ with U_I the tangential velocity, $y^+ = \frac{\rho y u^*}{\mu}$ the non-dimensional distance to the wall, ρ the density and u^* the friction velocity. Solving for u^* yields the shear stress $\rho(u^*)^2$.

Table 2. Wall boundary conditions

3.2 Meshing processes

The mesh used by Framatome for this simulation includes the following features.

- The cells used for meshing are trimmed, hexahedral cells, with local refinements especially around the grid surface.
- A prism layer mesher was used in order to resolve the turbulent boundary layer at the rod surface, two layers of prism cells were set on the wall surfaces. This prism layer thickness corresponds to the linear viscous sublayer, calculated thanks to the Dean correlation.
- Then, the mesh was extruded upwards and downwards of the grid to fully represent the bundle part of the geometry. The mesh is conformal between inlet and outlet faces for an immediate mapping of the flow field (pressure and velocity) to simulate periodic conditions at stated in Section 3.1.

The resulting mesh is composed of 35 million fluid cells.

Concerning EDF, the computational mesh (created with ICEM CFD v15.0, see Figure 4 (a) and (b) for some details) is composed of 42 million hexahedra and fully conformal. Even if such a mesh is difficult to create and time consuming, these mesh properties are extremely important, to not introduce numerical diffusion, which is not suitable for LES. It was verified *a posteriori* that the logarithmic wall function is active almost everywhere, except in some locations in the grid which complied with the wall-modeled LES carried out (globally $y^+>20$). The periodic top and bottom computational faces are also fully conformal. For more details about the numerics and the results, see [15].

Finally, in the version used by CEA for the present work, TrioCFD requires a tetrahedral mesh, which has the benefit of being easily generated in complex geometries such as the vicinity of the mixing grid of interest (see again Figure 4 (c) and (d) for details of the mesh within the grid), but also comes with a number of cells significantly higher than those proposed in the other simulation frameworks of the present paper (i. e. around 200 million tetrahedral elements, for an equivalent global refinement level). The criterion expressed in [7] of having 15 to 20 cells between two opposite walls is satisfied.

At this stage, no primastic layer can be implemented close to the walls with TrioCFD, yielding the need for an active wall function almost everywhere in the model.

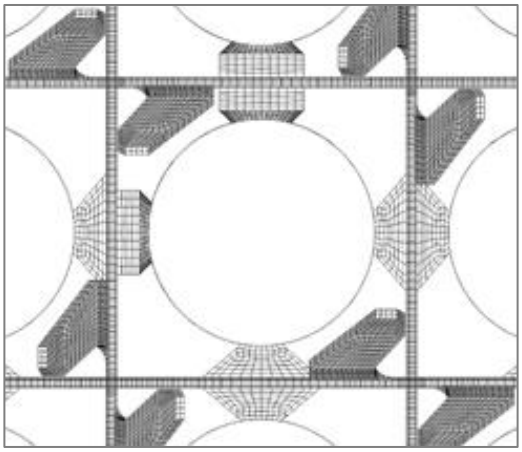

(a) EDF, *Code_Saturne*: mesh within the grid

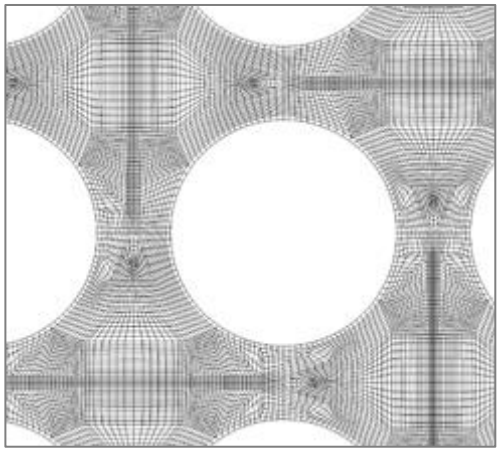

(b) EDF, *Code_Saturne*: mesh in the bare bundle region

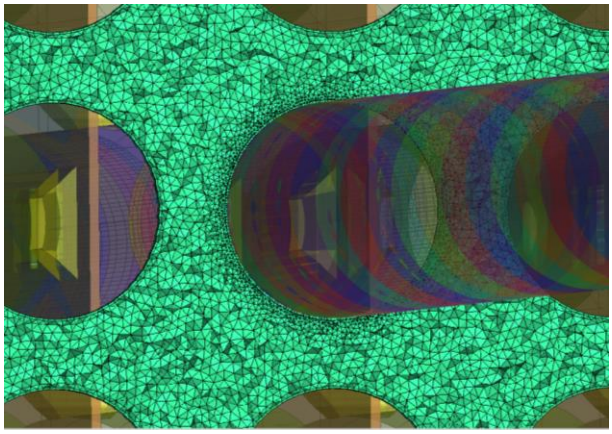

(c) CEA, TrioCFD: detail of the tetrahedral mesh within the bundle

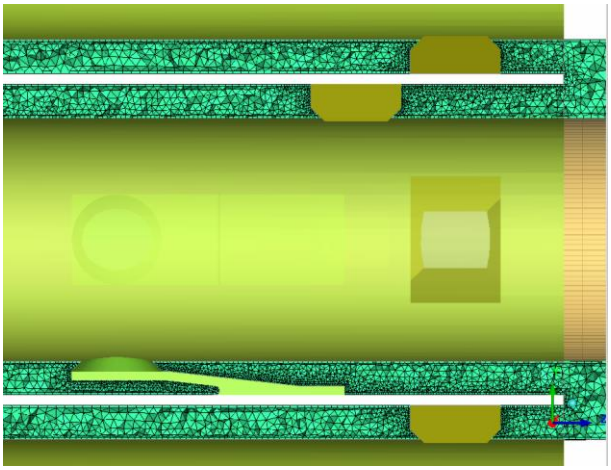

(d) CEA, TrioCFD: detail of the mesh in the vicinity of springs and dimples within the grid

Figure 4. Views of the meshes for *Code_Saturne* and TrioCFD

3.3 Turbulence modeling and numerical settings

Framatome and EDF use the Smagorinsky subgrid-scale model [8] (in its standard version for Framatome and its dynamic one for EDF) to model unresolved scales, whereas CEA uses the WALE (Wall-Adapting Local Eddy-viscosity) model [9], designed to have a sub-grid scale viscosity with the right asymptotic behavior in the near-wall region.

The main features of the various numerical methods are given in Table 3.

Framatome	EDF	CEA
Spatial discretization		
Finite volumes with cells of any shape (trimmed/hexa for Framatome and hexa for EDF)		Specific Finite Element/Finite Volume for tetrahedral cells (P0/P1 for pressure, P1NC for velocity)
Numerical features for the unsteady solver		
Second order implicit temporal discretization.	Smagorinsky constant varying from 0 to 0.065 Velocity and pressure coupling ensured via a predictor-corrector algorithm with three outer sub-iterations every time step Centered time discretization (Crank-Nicolson and Adams-Bashford) Second order spatial discretization with implicit gradient reconstruction to take into account non orthogonal faces Centered convection scheme with 2% of upwind in order to smooth pressure and velocity oscillations in the streamwise direction.	2^{nd} order Adams-Bashford explicit time integration Mixt 2^{nd} order (centered and upwind) for convection, centered second order for diffusion
Time-step and stability (CFL condition)		
Constant time-step of 5.10^{-4} s Mean CFL about 0.95	Constant time step equal to 10^{-5} s. Mean CFL about 0.94 Maximum CFL about 2.25	Constant time-step equal to 6.10^{-6} s Max CFL around 0.8
Parallel solution		
MPI	MPI & OpenMP [10]	Flat MPI

Table 3. Main numerical features in the different solvers

4 RESULTS AND CROSS-COMPARISONS WITH RESPECT TO EXPERIMENT

Figure 5 shows instantaneous 2D velocity vectors obtained with the different solvers 1 D_h and 2 D_h downstream of the mixing vane grid. The secondary transverse flows show clearly that the mixing vane is a split type one. The results are qualitatively in good agreement between the different models in terms of both intensity and location of the generated flows.

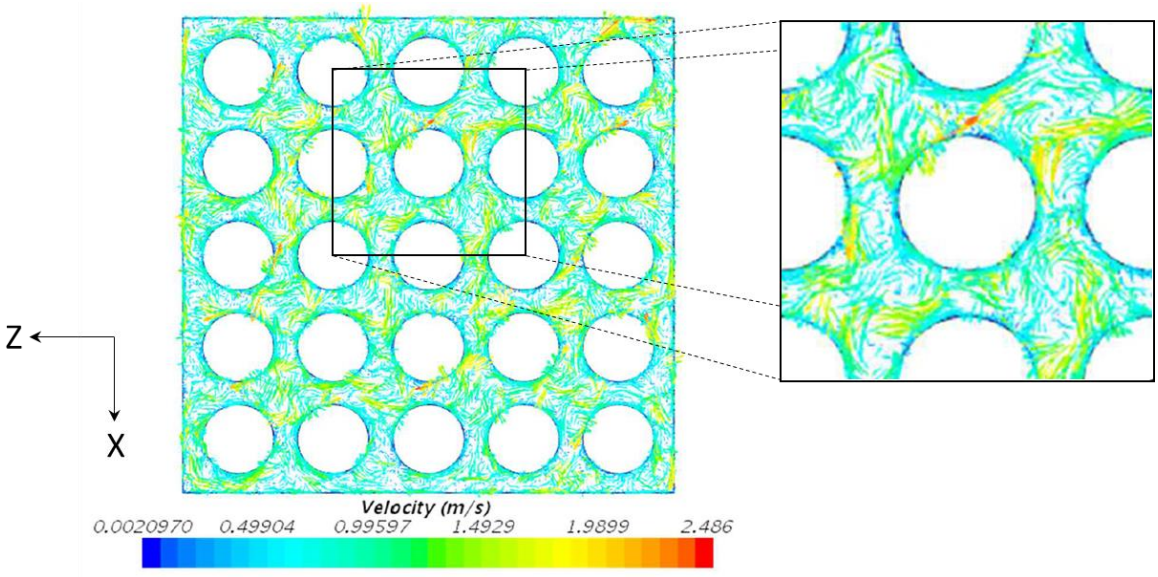

(a) Framatome, 1 D_h downstream of the grid

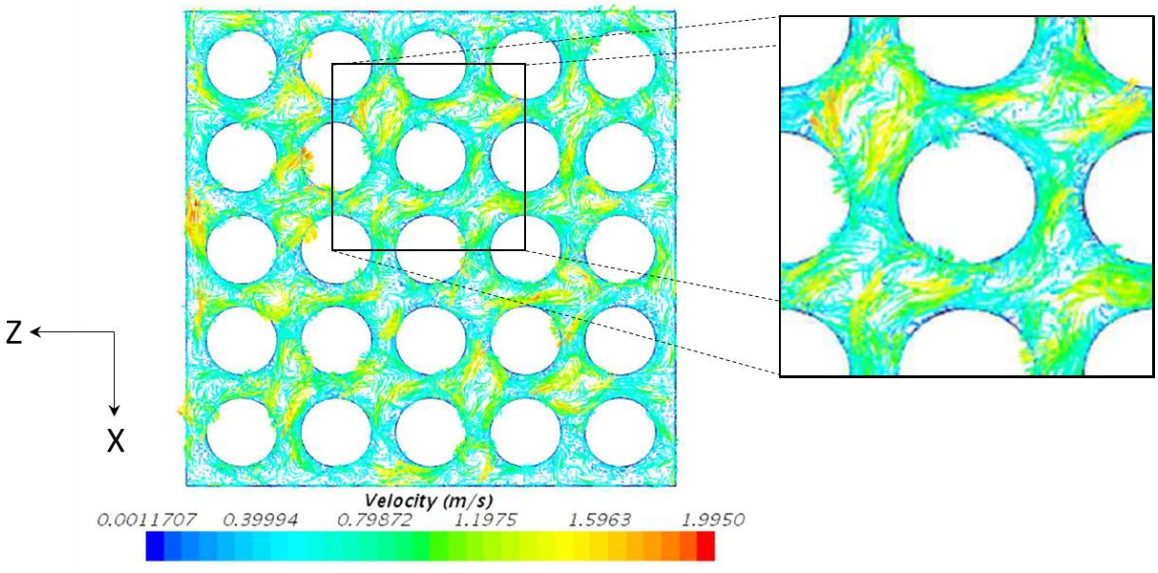

(b) Framatome, 2 D_h downstream of the grid

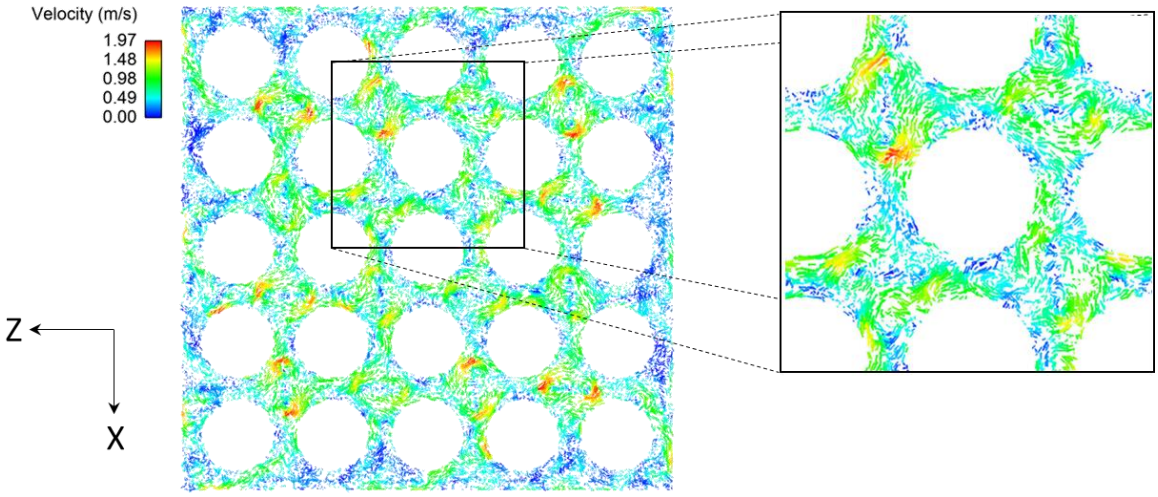

(c) EDF, 1 D_h downstream of the grid

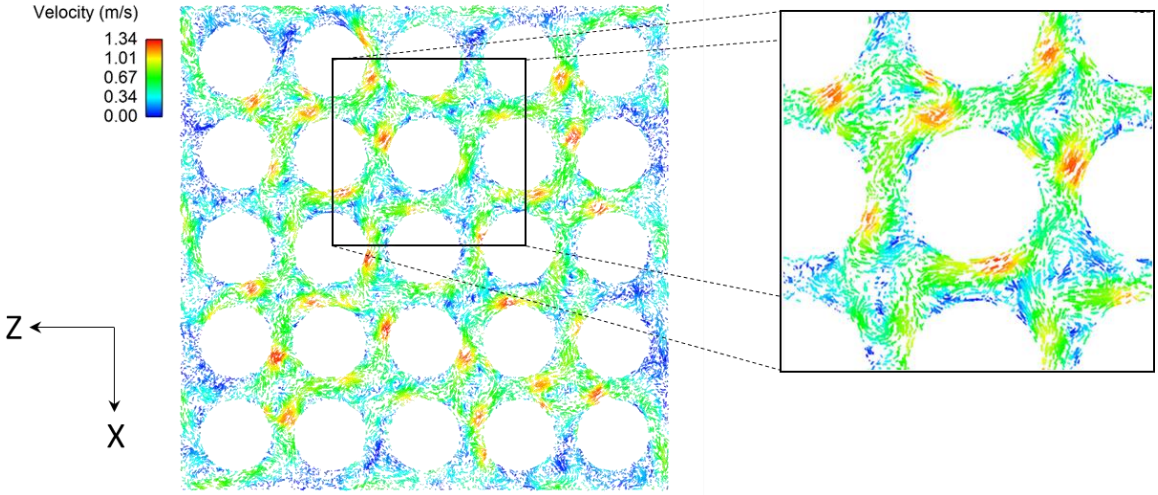

(d) EDF, 2 Dh downstream of the grid

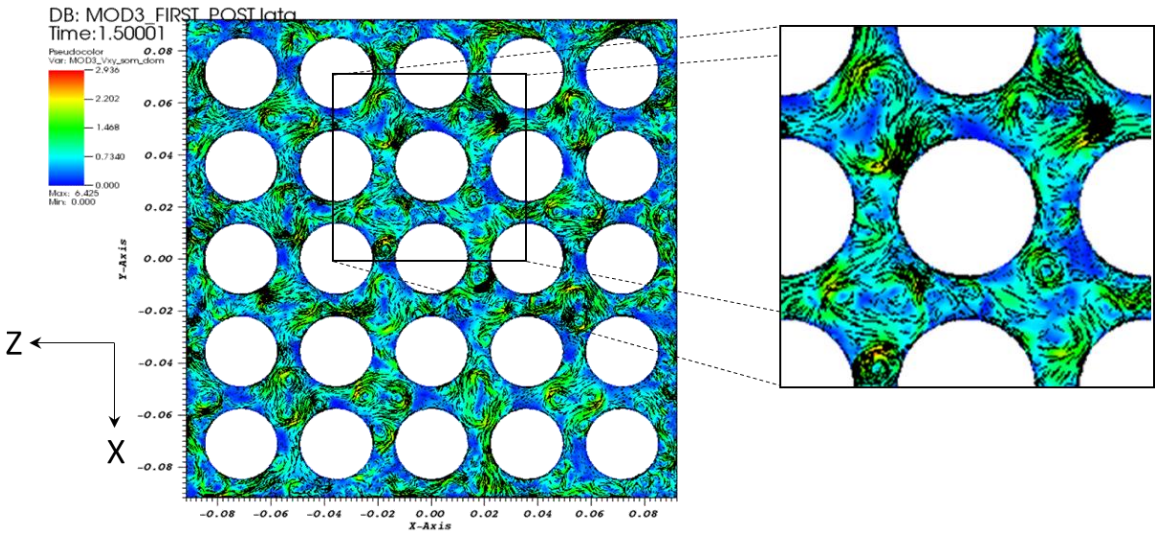

(e) CEA, 1 D_h downstream of the grid

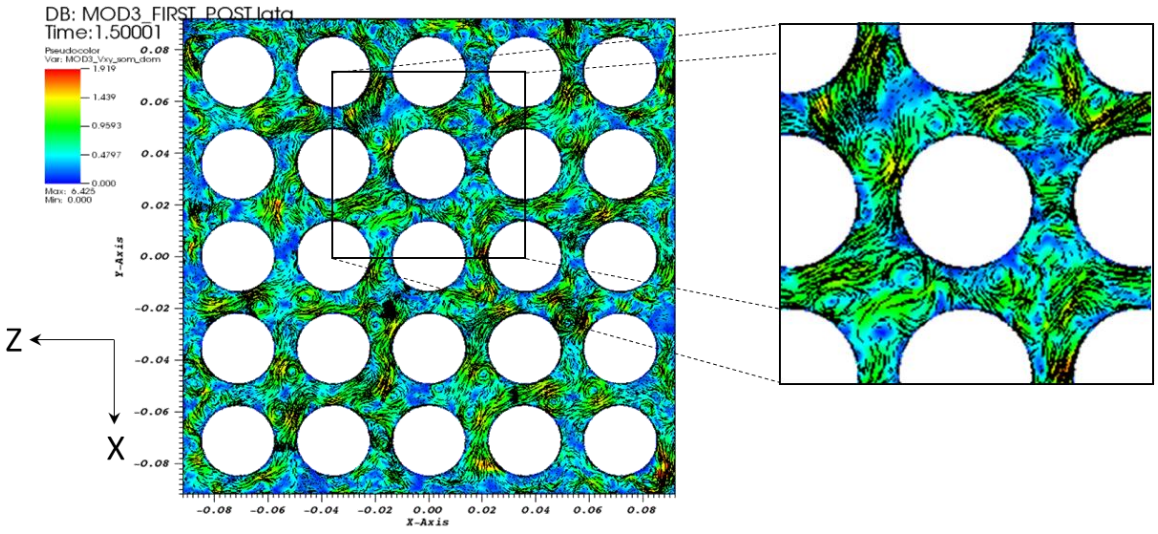

(f) CEA, 2 D_h downstream of the grid

Figure 5. Secondary transverse flow generated in the rod bundle downstream of the grid (colored by velocity in m/s)

The next paragraphs focus on specifically measured quantities, to compare the three numerical solutions to experimental measurements.

4.1 Velocity profiles downstream of the mixing grid

Vertical and cross velocities predicted by Star-CCM+, *Code_Saturne* and TrioCFD are plotted along line T1 displayed on Figure 6. The numerical predictions compared to LDV data are shown in Figures 7 and 8,

at 2 and 5 D_h downstream of the mixing grid, respectively. The laser lights the window on the left. The experimental profiles are only given for distances between 0 and 100 mm from sight window, due to measurement difficulties further away from the window. The vertical lines correspond to the positions of the rod symmetry axes.

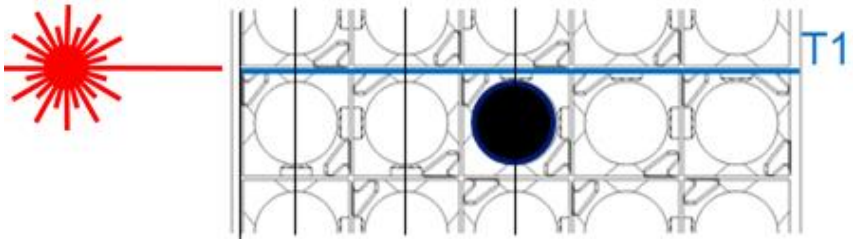

Figure 6. Location of line T1, laser is located on the left

Whatever the CFD code used, the overall agreement between numerical and experimental data is very satisfactory in the central region, for both components and both locations. Numerical results predicted by TrioCFD and Star-CCM+ are closer to experimental vertical velocities, especially at 5 D_h for Star-CCM+, whereas *Code_Saturne* is satisfactory at predicting the cross velocity. On the left side of the figures while approaching the casing, differences of behavior can be observed between the three numerical predictions and the experimental data due to the fact that the laser lights the window, which probably leads to distortion of experimental measurements.

Concerning the cross velocity, it can clearly be observed a change of sign (between -0.5 and 0.5 m/s) at 2 D_h from the grid, which indicates a very marked influence of mixing vanes near the grid, clearly predicted by the three CFD codes and measured by LDV. Further downstream at 5 D_h, the amplitudes of vertical and cross velocity oscillations decrease: the influence of mixing vanes naturally decreases. The flow tends toward a fully developed one in a bare bundle, after approximately 10 hydraulic diameters, although the traces of the secondary vortices are still perceptible (not shown here).

	Framatome / Star-CCM+	EDF / *Code_Saturne*	CEA / TrioCFD
$2D_h$	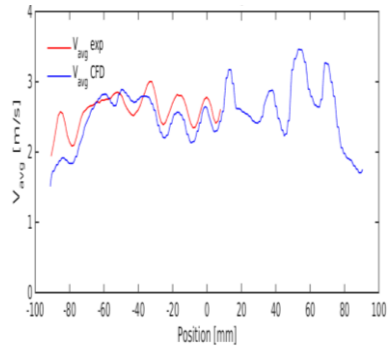	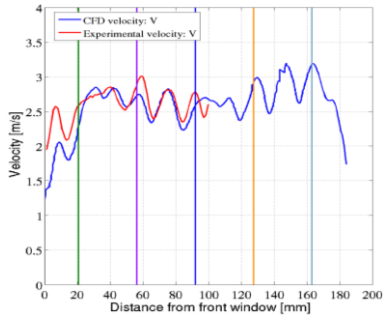	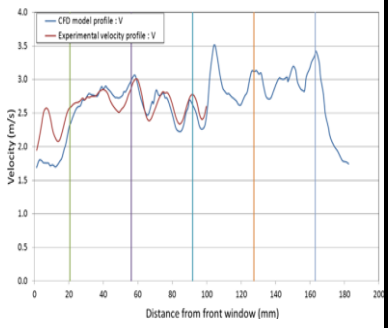
$5D_h$	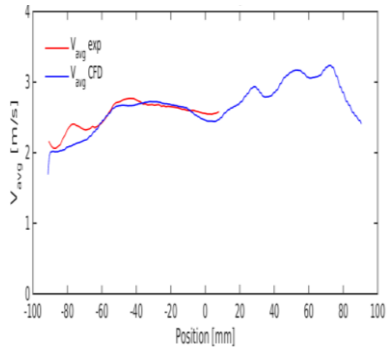	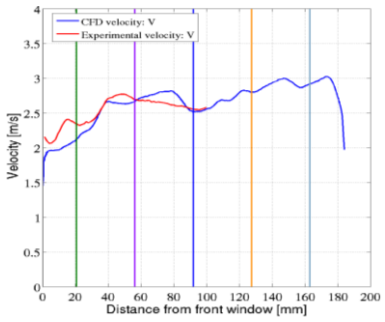	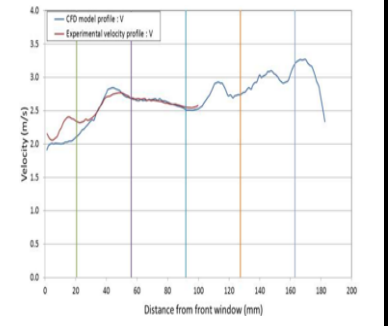

Figure 7. Vertical velocity profiles at 2 and 5 D_h along T1 for the three CFD code (in blue CFD velocity and in red experimental velocity)

	Framatome / Star-CCM+	EDF / *Code_Saturne*	CEA / TrioCFD
2D_h	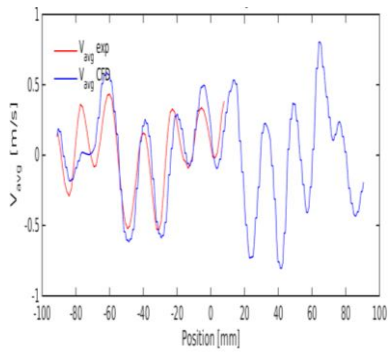	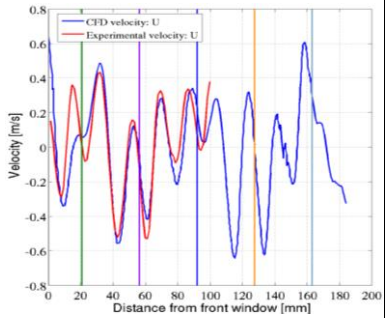	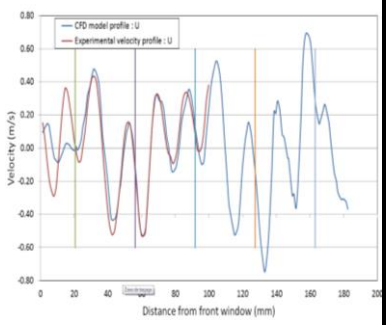
5D_h	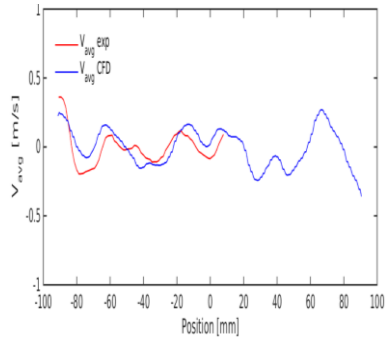	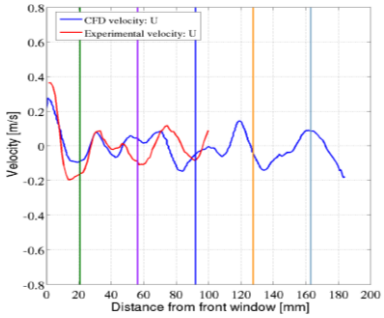	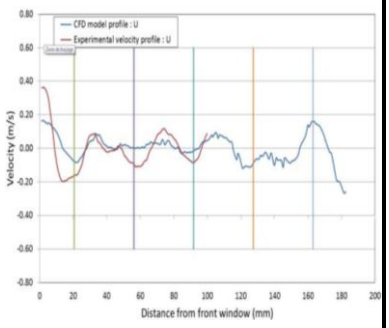

Figure 8. Cross velocity components profiles at 2 and 5 D_h along T1, for the three CFD codes (in blue CFD velocity and in red experimental velocity).

4.2 Pressure standard deviation distributions around the central rod

As stated in Section 2 and shown in Figure 2 for reference experimental results, unsteady pressure fluctuations measurements were performed around the central rod with a 10° increment. All three calculations were post-processed in order to compare the pressure standard deviation to experimental data thanks to polar representation. The comparison is presented at altitudes of 1 D_h, 2 D_h, 5 D_h and 10 D_h downstream of the mixing vane grid (see Figure 9).

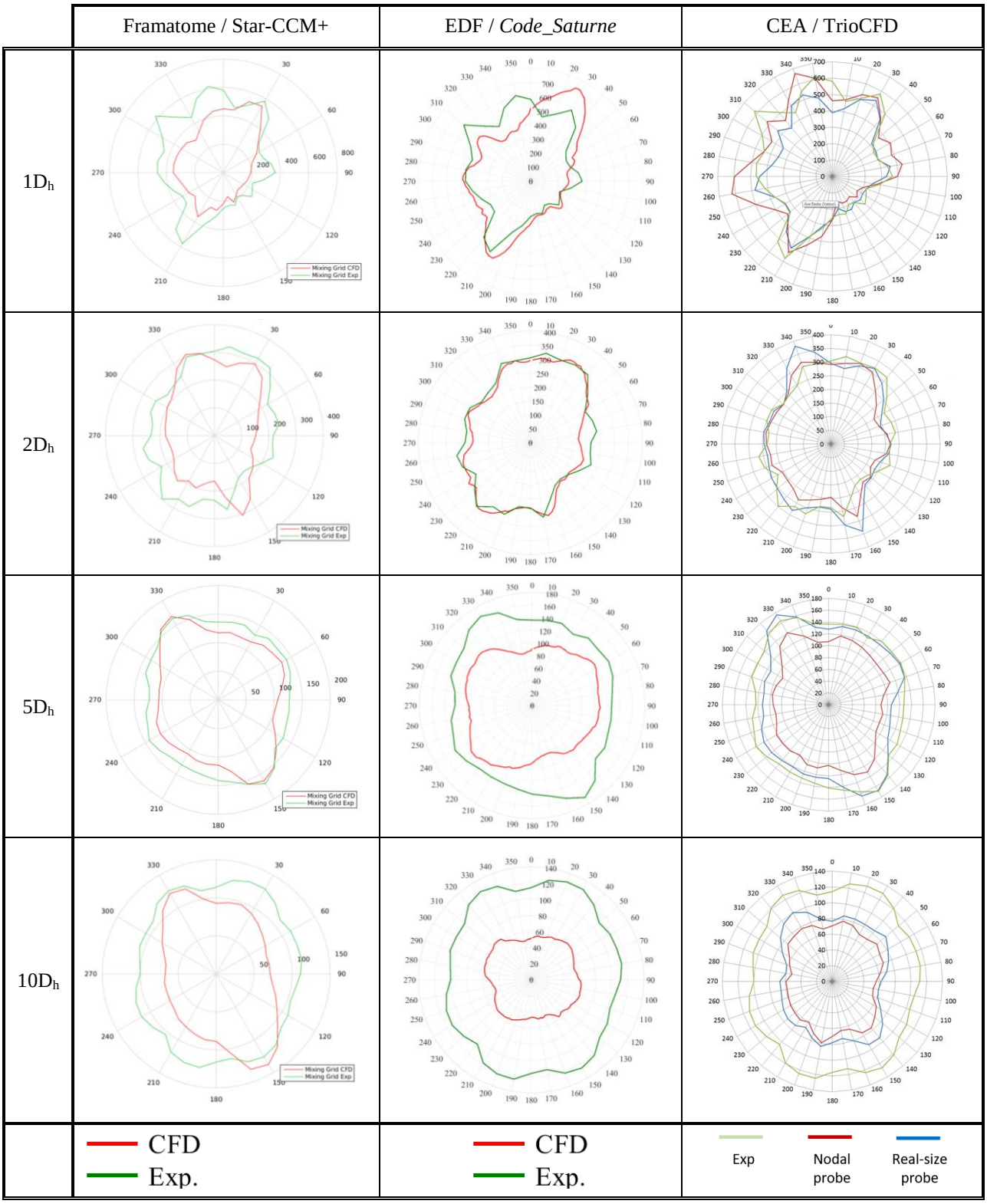

Figure 9. Polar representation of pressure standard deviation distribution around the central rod (red curves for CFD velocities, green curves for experimental velocities, blue curves do not have to be considered for this comparison)

For CEA, numerical results are provided for both nodal pressure probes and so-called real-size probes where the pressure is integrated over a surface representing the actual size of the experimental sensor. Only the results corresponding to nodal pressure probes, will be considered for the following. Real-size probes unexpectedly yield more filtered results, which has to be investigated in further work.

Results are here discussed in terms of azimuthal accuracy. Predictably, the pressure standard deviation azimuthal pattern is heavily polarized immediately after the mixing grid. This polarization is well reproduced by the codes in its (30° - 210°) diagonal, one hydraulic diameter downstream of the grid. The standard deviation pattern grows into a more homogeneous shape with altitude as well as it reduces in amplitude as the flow tends towards a fully developed flow in a bare bundle. All the solvers start drifting away from the experimental results at 5 D_h, mostly in amplitude. Some (150° - 330°) polarization still slightly persists at 5 D_h for Star-CCM+ and TrioCFD. This might be due to the use of wall functions for TrioCFD or *Code_Saturne*. DNS or a wall-resolved LES in all programs would provide more elements to conclude about this point.

4.3 Pressure standard deviation decay with respect to the distance downstream of the mixing grid

The decay of the pressure standard deviation around the central rod downstream of the mixing grid is plotted in Figure 10. The slope in the vicinity of the grid (up to 3 D_h downstream), where the standard deviation are the highest, is rather correctly reproduced by all the models. This is not the case going further away from the grid: if the change of slope around 4 D_h seen in the experiment is reproduced by the three simulations, the numerical results are inaccurate in all cases, yielding a decay after 5 D_h significantly faster than the experimental measurement.

5 DISCUSSION REGARDING LES VALIDATION AND RECOMMENDATIONS FOR FUTURE WORK TO CONSOLIDATE THE PROPOSED RESULTS

The simulations proposed in the current paper represent a significant computational effort to provide and compare best-estimate solutions in the CALIFS 5x5 configuration. Each proposed computational model, including its own meshing process, software choice and solver parameters, comes with some particular hypotheses clearly described in sections 3.1, 3.2 and 3.3. Models of this size are built in agreement with known recommendations, especially as far as mesh refinement is concerned and systematic *a posteriori* sensitivity and convergences studies are classically out of reach for simple reasons of requested computational power and time.

The first priority comment is that, whatever the mix of mesh characteristics and numerical solver, the obtained results are closed to each other and to the experiments up to 4 Dh downstream of the mixing grid. This applies to the azimuthal polarization of the pressure fluctuations where they are the most significant, the accurate reproduction of secondary cross flows in the tube bundle and the decay of the pressure standard deviation. The second comment is that all computational models fail at reproducing the correct decay of the pressure fluctuations after 5 Dh downstream of the mixing grid.

While still not fully understood at this stage, this discrepancy in the agreement between experiment and simulation seems to suggest that some persistent structures in the flow are missed in the numerical models, which could be low frequency vortices generated by the vanes whose influence is masked by high frequencies turbulent structures correctly captured just after the grid, or due to the use of wall functions which filter the turbulence created by the walls.for *Code_Saturne* or TrioCFD

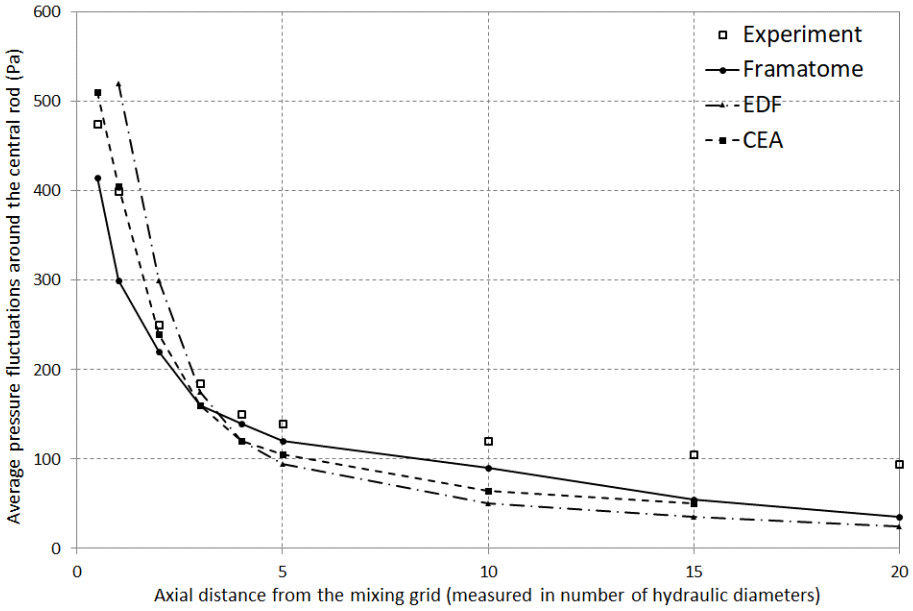

Figure 10. Pressure standard deviation decay downstream of the mixing grid

One strategy to address the remaining issue and go further the generally positive results obtained in the proposed work would be to complement this study with sensitivity analyses to try to identify the modeling components actually influencing the decay of the pressure fluctuations. The parameters to deal with could principally be the mesh refinement, both in the wall normal direction and in the axial direction of the bundle, and the models to account for the velocity profile in the boundary layer, up to a fully resolved and validated solution close the walls to serve as a reference. This work should certainly be performed with less power

consuming models, obtained for instance after a reduction of the Reynolds number, to allow the efficient production of series of calculation in a reasonable time. It obviously implies that some new experimental results are obtained at these lower Reynolds numbers and that discrepancies of the same nature are still observed in these less challenging conditions. Advanced hybrid RANS/LES approaches, as introduced in paragraph 3.1, should be worth testing in this prospective work, especially in the case where the fully resolved velocity field close to the walls proves preponderant.

6 CONCLUSION

The proposed advanced benchmark involving three CFD software solutions provides significant insights related to the maturity of CFD simulation for single phase highly turbulent flows in rod bundles equipped with one or more mixing grid(s), representative of the need for fretting assessment in PWR reactor and other design applications involving in-core hydraulics.

One major lesson is that very satisfactory results are globally obtained with all the models independently from the modelling options introduced above, suggesting that the software offer for this kind of calculations has reached a generic and significant level of robustness, accuracy and maturity. This comes with a mandatory prerequisite that the suitable expertise is mobilized in model building and tuning of numerical parameters associated to the chosen method for time and space discretization.

Some discrepancies yet remain regarding the reproduction of the pressure standard deviation decay far downstream of the mixing in the present case. It opens research topics to identify the origin of these differences between simulation and experiment, especially to state if they are likely to reappear in other configurations with more significant effects, like for the complex hydraulic situation at the bottom of a PWR fuel assembly, with incoming jets from the main water supply impacting the nozzle with consequences on the turbulent flow through the bundle and the first holding grid above.

References

1. “Review of Fuel Failures in Water Cooled Reactors”, IAEA Nuclear Energy Series NF-T-2.1 (2010).

2. M.P. Païdoussis, “A review of flow induced vibrations in reactors and reactor components. Nuclear Engineering and design 74, 31-60 (1982).

3. F. Moreno, B. Collard, V. Faucher, “Measurement of fluctuating fluid pressure exerted on the walls of tube bundle”. Flow Induced Vibrations, The Hague, Netherlands, 2016.

4. F. Moreno, S. Bantiche, F. Bazin, T. Lohez, D. Picard, S. Testanière, L. Rossi, “Unsteady Pressure and Velocity Measurements in 5x5 Rods Bundle Using Grids With and Without Mixing Vanes”. 12th International Topical Meeting on Nuclear Reactor Thermal-Hydraulics, Operation and Safety, Qindao, China, 2018.
5. P. Sagaut, “Large Eddy Simulation for Incompressible Flows (Third ed.)”. Springer, 2006.
6. S. Delafontaine, “Simulation of unsteady fluid forces on a single rod downstream of mixing grid cell”. Nuclear Engineering and Design, vol. 332, 2018.
7. Best practice Guidelines for the use of CFD in Nuclear Reactor Safety Application, Collective document, 2007, OECD Nuclear Energy Agency, Committee on the Safety of Nuclear Installations, NEA/CSNI/R-2007-5.
8. M. Germano, U. Piomelli, P. Moin, W. Cabot, “A dynamic subgrid-scale eddy viscosity model”, Physics of Fluids, vol. 3(7), 1991.
9. F. Ducros, F. Nicoud, “Subgrid-scale stress modelling based on the square of the velocity gradient tensor”. Flow Turbulence and Combustion, vol. 62(3), 1999.
10. Y. Fournier, J. Bonelle, C. Moulinec, Z. Shang, A.G. Sunderland, J.C. Uribe, “Optimizing Code_Saturne computations on Petascale systems”. Computers & Fluids, vol. 3(7), 2011.
11. Benhamadouche, S., Moussou, P., Le-Maître, C., 2009. CFD estimation of the flow-induced vibrations of a fuel rod downstream a mixing grid. Proceedings of PVP 2009 ASME Pressure Vessels and Piping 2009 / Creep 8 Conference, July 22-26, Prague, Czech Republic.
12. D. Wells and Y. Hassan, “Overview of CFD Round Robin Benchmark of the High Fidelity Fuel Rod Bundle NESTOR Experimental Data”, The 16th International Topical Meeting on Nuclear Reactor Thermal Hydraulics (NURETH-16) , Hyatt Regency Chicago, Chicago, IL, USA, August 30-September 4 (2015).
13. S. Benhamadouche. On the use of (U)RANS and LES approaches for turbulent incompressible single phase flows in nuclear engineering applications. *Nuclear Engineering and Design*, 312, pp. 2-11 (2017)
14. Piomelli, U., 2008. Wall-Layer Models for Large-Eddy Simulations. Progress in Aerospace Sciences, Large Eddy Simulation - Current Capabilities and Areas of Needed Research, 44, no. 6 : 437–46.
15. Benhamadouche, S., Gauffre, M.-C., Badel, P. Wall-modelled large eddy simulation of the flow through PWR fuel assemblies AT ReH=66,000 - Validation on califs experimental setup, International Topical Meeting on Advances in Thermal Hydraulics, ATH 2018 - Embedded Topical Meeting pp. 765-776, 2018.
16. U. Bieder, F. Falk, G. Fauchet, Les analysis of the flow in a simplified pwr assembly with mixing grid, Progress in Nuclear Energy 75 (2014) 15 – 24.
17. G. Chen, Z. Zhang, Z. Tian, X. Dong, Y. Wang, Cfd simulation for the optimal design and utilization of experiment to research the flow process in pwr, Annals of Nuclear Energy 94 (2016) 1 – 9.
18. J. Xiong, R. Cheng, C. Lu, X. Chai, X. Liu, X. Cheng, Cfd simulation of swirling flow induced by twist vanes in a rod bundle, Nuclear Engineering and Design 338 (2018) 52 – 62.
19. U. Bieder, F. Falk, G. Fauchet, Cfd analysis of the flow in the near wake of a generic pwr mixing grid, Annals of Nuclear Energy 82 (2015) 169 – 178.
20. Z. Karoutas, C. Gu, B. Scholin, 3-d flow analyses for design of nuclear fuel spacer, Proceedings of the Seventh International Meeting on Nuclear Reactor Thermal-Hydraulics (1995) 3153–3174.

21. W.-K. In, D.-S. Oh, T.-H. Chun, Flow analysis for optimum design of mixing vane in a pwr fuel assembly, Nuclear Engineering and Technology 33 (2001).
22. S. Cheng, H. Chen, X. Zhang, Cfd analysis of flow field in a 5x5 rod bundle with multi-grid, Annals of Nuclear Energy 99 (2017) 464 – 470.
23. J. R. Lee, J. Kim, C.-H. Song, Synthesis of the turbulent mixing in a rod bundle with vaned spacer grids based on the oecd-kaeri cfd benchmark exercise, Nuclear Engineering and Design 279 (2014) 3 – 18.